

# ShearWave™ Elastography Improves the Management of Patients with Breast Lesions



Prof Boris Brkljačić, Department of Diagnostic and Interventional Radiology, University Hospital “Dubrava”, University of Zagreb School of Medicine, Zagreb, Croatia.

Prof Chang Cai, Department of Ultrasound, Fudan University Shanghai Cancer Center; Department of Oncology, Shanghai Medical College, Fudan University, Shanghai, P. R. China.

Dr André Farrokh, Universitätsklinikum Schleswig-Holstein, Kiel, Germany.

Dr Smriti Hari, Department of Radiology, All India Institute of Medical Sciences, New Delhi, India.

Dr Gordana Ivanac, Department of Diagnostic and Interventional Radiology, University Hospital “Dubrava”, University of Zagreb School of Medicine, Zagreb, Croatia.

Dr Laurent Lévy, Breast Imaging Unit, Paris Radiology Institute (IRP), Paris, France.

Dr Nicolas Perrot, Pyramides Medical Imaging Center, Paris, France.

Prof Fritz Schäfer, Universitätsklinikum Schleswig-Holstein, Kiel, Germany.

Dr Christophe Tourasse, Radiology Department, Jean Mermoz Private Hospital, Lyon, France.

Dr Chen Ya-Ling, Department of Ultrasound, Fudan University Shanghai Cancer Center; Department of Oncology, Shanghai Medical College, Fudan University, Shanghai, P. R. China.

## Contents

1. Introduction
2. Reliability of ultrasound breast cancer risk assessment
  - 2.1 “Almost perfect” repeatability of SWE™ images and measurements
  - 2.2 Improved inter-observer agreement on cancer risk assessment of breast masses with ultrasound
3. Consistent stiffness values of breast tissue and lesions
  - 3.1 Stiffness of normal breast tissue
  - 3.2 Stiffness values of breasts lesions
4. Improved diagnosis of breast cancer
  - 4.1 Reduction of false positives of breast ultrasound
  - 4.2 Improved sensitivity of breast ultrasound
5. Information for treatment planning and monitoring
  - 5.1 Pre-operative assessment of breast cancer size
  - 5.2 Cancer aggressiveness and prognostic information.
    - 5.2.1 Stiffness and histo-pathologic severity
    - 5.2.2 Stiffness and cancer aggressiveness
    - 5.2.3 Stiffness and immuno-histochemical phenotype
  - 5.3 Monitoring and prediction of response to neo-adjuvant chemotherapy
6. Conclusion
7. References

Acknowledgements: Wendie A. Berg, MD, Department of Radiology, Magee-Womens Hospital of UPMC, University of Pittsburgh School of Medicine, Pittsburgh, PA, USA et Claudia Kurtz, MD, Radiologie und Nuklearmedizin, Luzerner Kantonsspital, Luzerne, Suisse.

# 1. Introduction

Owing to its recognized clinical utility, ultrasound imaging has been fully integrated into routine practice at different phases of the management of patients with breast lesions patients, including breast masses characterization, biopsy guidance, follow-up of probably benign masses, axillary lymph nodes examination, and surgical planning [1-3]. In addition, recent results demonstrated the significant contribution of breast ultrasound imaging in screening for mammographically occult cancers [4-5]. However, breast ultrasound imaging suffers from some limitations.

Despite the development of the Breast Imaging-Reporting and Data System (BI-RADS®) for ultrasound developed by the American College of Radiology (ACR), the standardization of breast ultrasound exams and of the reporting on findings can still be challenging. Several works reported poor inter-observer agreement for the overall malignancy risk assessment on ultrasound, especially for BI-RADS 3 and 4 masses [6].

When used for breast lesion characterization, ultrasound benefits from a high sensitivity (usually above 90% for invasive cancers) and negative predictive value (NPV; above 90%). However, as many as 40-50% of biopsies prompted by grayscale ultrasound are for benign lesions, which therefore could be avoided [1]. In parallel, theoretically less than 2% of BI-RADS 3, probably benign lesions, proves ultimately to be malignant, some of those being high-grade invasive cancers, which mimic cysts or complicated cysts with debris. Therefore, an early identification and biopsy of those few malignancies, instead of short-term follow-up, could obviously improve treatment outcomes.

In biopsy-proven cancers, ultrasound usually underestimates the measurement of tumor size, and the pre-operative ultrasound examination of the axilla in search for metastatic lymph nodes tend to suffer from reduced sensitivity (42% in a recent large scale experience [7]).

As the place and role of ultrasound imaging tends to increase for breast cancer screening purposes, an obstacle to its widespread use as a screening tool is the very high number of false positives [4-5]. ShearWave™ Elastography (SWE™) based on supersonic shear imaging can measure and map tissue stiffness in real-time and has proven to be a valuable adjunct to conventional ultrasound imaging. It can fully integrate routine ultrasound breast examinations, with little extra examination time for patients and physicians.

Furthermore, it has been demonstrated by close to 100 clinical studies and peer-reviewed publications that breast tissue and breast lesion stiffness information helps address most of the limitations of breast ultrasound.

---

## 2. Reliability of Breast Cancer Risk Assessment with Ultrasound

The addition of any new radiological information to the highly-standardized BI-RADS® classification requires that both the acquisition and the interpretation of the new information demonstrate high reproducibility and reliability, even though inter-observer agreement on some BI-RADS features and assessments may only be fair [6].

Although the measurement of tissue stiffness is affected by the level of compression that is applied to the tissue [8], using standardized technique and after training on 10 cases, Cosgrove et al reported excellent reproducibility results from the prospective Breast Elastography 1 (BE1) multinational study, which was run at 16 sites in Europe and the USA [9].

Several other studies have reported almost perfect intra-operator reproducibility and moderate to substantial interobserver agreement [10-15], and 3 studies even reported improved inter-observer agreement on breast cancer risk assessment by adding SWE™ evaluation to grayscale evaluation (Table 1) [11;13;16]. Contrary to what can be performed in experimental settings, both an absolute lack of pressure and excessive compression of tissue rarely occur in routine clinical practice because of the need for minimal compression to produce good quality images without causing patient harm or discomfort.

| Author     | BI-RADS | BIRADS + SWE™ |
|------------|---------|---------------|
| Gweon [11] | 0.69    | 0.82          |
| Lee [13]   | 0.56    | 0.65          |
| Youk [16]  | 0.38    | 0.80          |

**Table 1. Increase of inter-observer agreement (kappa value) on overall cancer risk assessment of breast masses by the addition of SWE™ evaluation to BI-RADS assessment.**

## 2.1 “Almost perfect” repeatability of SWE™ images and measurements

Cosgrove et al compared 3 consecutive SWE™ acquisitions of 758 breast masses visible on ultrasound imaging. In 88% of the cases, the 3 SWE™ images were evaluated qualitatively to be very or reasonably similar, whereas they were found to be dissimilar in only 8/758 masses (1%). In the remaining 84 masses (11%), 2 out of 3 images were evaluated to be of similar appearance.

Although this outcome was significantly impacted by the irregularity of masses on grayscale imaging and by presence of malignancy, rates of dissimilar acquisitions remained very low (1.6% for irregular masses and 3.5% for malignant masses) [9].

The intra-operator reproducibility of size and stiffness measurements performed on the 3 SWE™ images was calculated with Intraclass Correlation Coefficients (ICC).

The reproducibility of size measurements (longest diameter, perimeter and calculated area) was almost perfect with ICC of at least 0.94, while stiffness measurements showed substantial to almost perfect reproducibility, with ICC ranging from 0.71 (E<sub>min</sub>) to 0.87 (E<sub>mean</sub>). Size and stiffness measurements appeared to be more reproducible on benign than malignant masses, although ICCs were still almost perfect (0.92) for size measurements and substantial for E<sub>mean</sub> (0.71) in cancers [9].

## 2.2 Improved inter-observer agreement on cancer risk assessment of breast masses with ultrasound (Table 1)

Variability of interpretation of breast ultrasound images exists, despite standardization of reporting of ultrasound findings.

Reducing variability is desirable in clinical practice. In their study on 758 breast masses with grayscale ultrasound imaging and SWE™, Cosgrove et al investigated the inter-observer agreement of the reading of ultrasound and SWE™ images, with a blind review performed by an independent expert reviewer.

For each of the 758 masses, 3 grayscale features and 3 elastographic features were assessed by the reviewer and was compared to initial assessment. Inter-observer agreement was calculated with weighted kappa, and the highest value (k=0.66) was obtained for evaluation of the maximum stiffness of the masses. In contrast, agreement was lower for all grayscale features: k=0.58 for mass shape, k=0.53 for mass orientation and k=0.38 for mass margins. Interobserver agreement on BI-RADS assessments was moderate (k=0.59) and poor for each of the individual BI-RADS classes 3, 4a, 4b and 4c (k≤0.17) [9]. Interobserver agreement on BI-RADS assessments was lower than the agreement on maximum stiffness.

The potential of SWE™ to improve consistency of sonographic assessment of breast masses was further supported by 3 other studies. Gweon et al evaluated 153 breast masses for inter-observer agreement of the BI-RADS assessment and qualitative SWE™ features between 2 experienced radiologists who performed a blind review of images acquired by other experts [11].

The agreement was substantial for the BI-RADS score (k=0.69), for the color evaluation of maximum stiffness (k=0.79), for the homogeneity of the SWE™ map (k=0.77) and for the SWE™ pattern classification developed by Tozaki et al [17] (k=0.64). It was only moderate for the shape of the SWE™ map (k=0.56).

The most reproducible combination of grayscale and SWE™ assessment providing almost perfect agreement consisted in the combination of BI-RADS and maximum stiffness (k=0.82).

Similarly, Lee Et Al [13] Demonstrated on 219 breast masses an increase of the inter-observer agreement of the global ultrasound evaluation of breast masses, when both BI-RADS and SWE™ assessments were combined.

The evaluation of SWE™ images consisted in a combination of both homogeneity information and maximum stiffness, in one scanning plane or in two orthogonal scanning planes. The inter-observer agreement was calculated using the readings from 5 blinded radiologists. Kappa values increased from 0.56 with BI-RADS alone to 0.63 and 0.65, by combining elastographic evaluation in one and two scanning planes, respectively. The agreement between the 5 readers on the SWE™ assessment alone was  $k=0.76$  with either one or two scanning planes. Youk et al investigated the added value of 3D ultrasound imaging with and without SWE™ as compared to 2D grayscale imaging [16]. On the population of 163 breast lesions scheduled for ultrasound-guided biopsy, the inter-observer agreement for some of the grayscale features was increased by the addition of 3D evaluation: mass shape (increase from  $k=0.61$  to  $k=0.84$ ), mass orientation (increase from  $k=0.62$  to  $k=0.89$ ), and posterior acoustic features (increase from  $k=0.57$  to  $k=0.78$ ). The agreement on the overall cancer risk assessment using the BI-RADS score was not improved ( $k=0.38$ ). The agreement on the overall cancer risk assessment increased from  $k=0.38$  to  $k=0.80$  and  $k=0.73$  by adding 2D-SWE™ and 3D-SWE™ features respectively. The slight decrease of the kappa value with 3D-SWE™, as compared to 2D-SWE™, was most probably because the assessment of SWE™ homogeneity did not show the same level of agreement in 3D ( $k=0.63$ ) as compared with 2D ( $k=0.99$ ).

## 3. Consistent Stiffness

Since the publication of the first prospective study on 48 mammographically occult non-palpable lesions detected at ultrasound [18], the average stiffness values of breast tissue and lesions have been reported by several independent studies, in different clinical settings and on different populations, thus providing a complete overview of breast stiffness.

### 3.1 Stiffness of normal breast tissue

The stiffness values of normal breast tissue have been established to be between 3 and 9 kPa in fatty tissue, and between 11 and 50 kPa in fibroglandular tissue [18-20].

Rzyski et al specifically designed their study to evaluate the variations of stiffness values in both glandular and fatty breast tissue in healthy subjects depending on several clinical and physiological factors. In 101 women of mean age 43 years, mean stiffness in the breast gland was  $11.28\pm 5.79$  kPa, while it was  $9.24\pm 4.48$  kPa in fatty tissue. Statistically significant differences were observed between inner and outer quadrants for both glandular ( $12.4\pm 6.4$  kPa versus  $10.9\pm 8.3$  kPa, respectively) and fatty tissue ( $10.6\pm 5.3$  kPa versus  $8.1\pm 4.7$  kPa, respectively). The stiffness of glandular tissue was found to correlate positively with age, whereas stiffness of fatty tissue correlated positively with the overall duration of lactation [19].

### 3.2 Stiffness values of breast lesions

Significant differences in stiffness values between benign and malignant breast lesions have been reported by 13 studies (Table 2 and Figure 1). On average, malignant lesions were found to be 3.7 times stiffer than benign lesions, with a cancer/benign stiffness ratio ranging from 2.3 [13] to 5.3 [21]. The average stiffness value of benign lesions never exceeded 60 kPa and was equal to or below 50 kPa in 11/13 studies. In contrast, the average stiffness value of malignant lesions was found to be above 100 kPa in all studies, and even above 130 kPa in 12 of them.

| Author              | Nb lesions | Mean age (years) | Stiffness of cancers (kPa) | Stiffness of benign masses (kPa) | Stiffness ratio cancer/benign |
|---------------------|------------|------------------|----------------------------|----------------------------------|-------------------------------|
| Athanasίου [18]     | 48         | 58               | 146.6+/-40.05              | 45.3+/-41.1                      | 3.2                           |
| Au [21]             | 123        | 49               | 130.7+/-84.1               | 24.8+/-22.1                      | 5.3                           |
| Berg [22]           | 939        | 52               | 179                        | 41                               | 4.4                           |
| Berg [23]           | 1562       | 52               | 180                        | 43                               | 4.2                           |
| Chang [24]          | 182        | 48               | 153.3+/-58.1               | 46.1+/-42.9                      | 3.3                           |
| Chang [25]          | 150        | 48               | 150+/-52.3                 | 47.3+/-44.3                      | 3.2                           |
| Dobruć-sobczak [26] | 84         | 54               | 145.7                      | 41.1                             | 3.6                           |
| Ko [27]             | 34         | 46               | 107.5+/-74.6               | 42.6+/-30.4                      | 2.5                           |
| Lee [13]            | 156        | 44               | 137.4+/-68.5               | 59.2+/-91.1                      | 2.3                           |
| Tanter [20]         | 15         | 53               | 179+/-41                   | 55+/-21                          | 3.3                           |
| Tozaki [17]         | 100        | 54               | 146+/-80                   | 42+/-28                          | 3.5                           |
| Youk [28]           | 389        | 46               | 157.5                      | 40.5                             | 3.9                           |
| Youk [14]           | 130        | 47               | 140.7+/-58.5               | 34.8+/-17.7                      | 4.0                           |

Table 2. Average+/-SD or median (Berg) values of maximum stiffness of benign and malignant breast lesions, measured as the mean or maximum (Berg) value within the ROI placed over the stiffest area in or adjacent to the lesions.

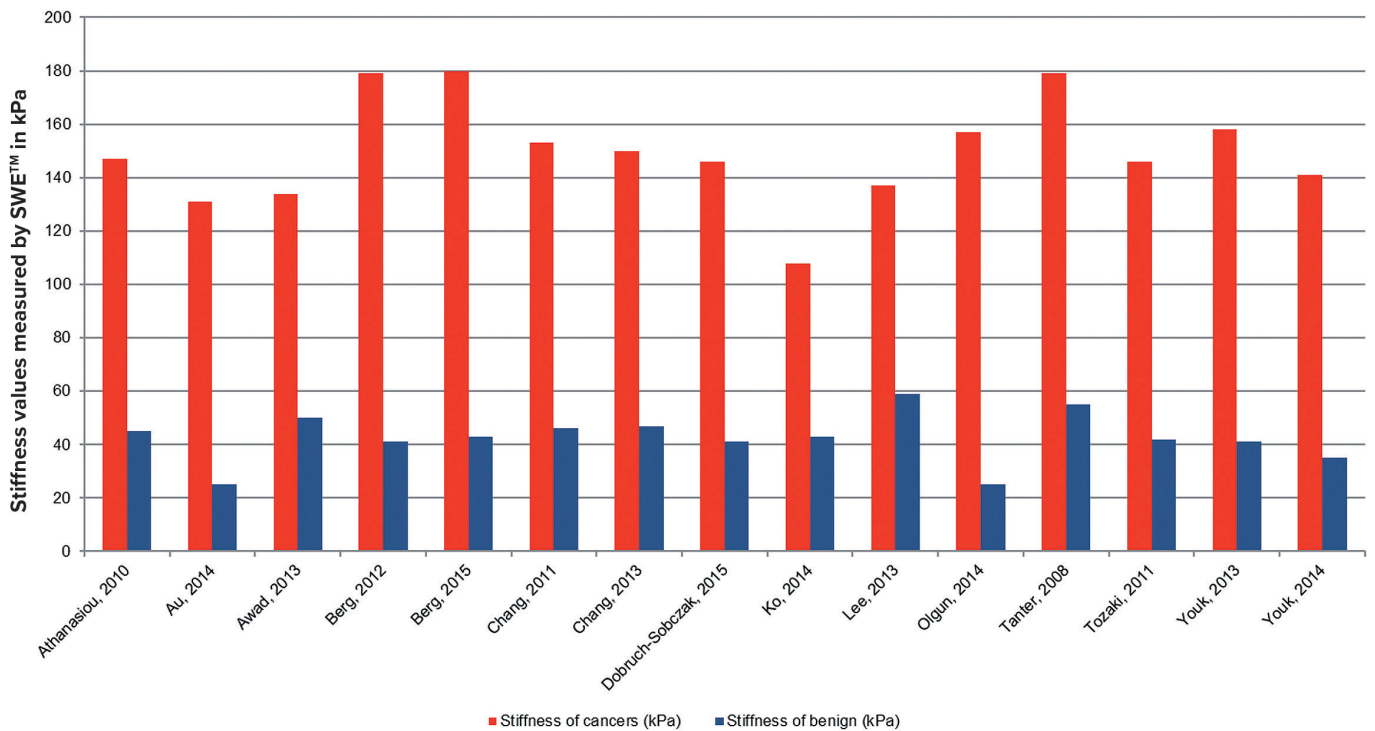


Figure 1. Average values of breast lesions maximum stiffness across 13 peer-reviewed publications according to their pathological status (benign or malignant).

## 4. Improved Diagnosis of Breast Cancer

Breast ultrasound has long been recognized as the method of choice for the characterization of symptomatic and/or screen-detected breast lesions, owing to its high sensitivity and NPV. However, it suffers from average specificity and positive predictive value (PPV) usually reported to be in the range of 40-60% in the context of breast lesion characterization [6], and even lower (around 10-20%) for ultrasound screening of breast cancer [4].

The overall difference in stiffness between benign and malignant breast lesions has been initially proposed as a potential additional differentiating factor that could improve the global evaluation of breast cancer risk by ultrasound imaging [18;20]. Indeed, by providing complementary stiffness information, the evaluation of breast lesions with SWE™ proved to complement the morphological assessment of the malignancy risk. This proved to be especially true for oval, circumscribed breast masses with no other suspicious features on grayscale imaging. In these probably benign and low suspicion masses, SWE™ evaluation could help eliminate false negative cases, while still significantly reduce false positive cases [22].

When stiffness had been considered as the only criterion for malignancy risk assessment, diagnostic performances of SWE™ showed an increase in specificity as compared to the BI-RADS® evaluation, with a concomitant decrease in sensitivity [17; 29-30]. In these studies, the BI-RADS® classification sensitivity was reported to be perfect (100%) while specificity was very low in the context of breast lesion characterization (38.7% [17] and 14.3% [29]), which may highlight a possible bias in patients' recruitment. Kim and Yoon focused their analyses on the identification of factors associated with false positive and false negative outcomes of SWE™. Lesion size and depth [29], breast thickness [29-30], patients' age [30], the presence of an echogenic halo on grayscale ultrasound [30] were found to be correlated with higher risks of false diagnosis with SWE™. These results have highlighted the need to consider these parameters when interpreting stiffness images and information; however, none of these studies evaluated the combination of lesions BI-RADS assessment with SWE™ information.

### 4.1 Reduction of false positives of breast ultrasound

The ability of SWE™ assessment to increase the specificity and the PPV for biopsy recommendation of breast ultrasound has been demonstrated by an increasing number of studies in the context of diagnostic ultrasound (Figures 2 and 3). By selectively reconsidering the decision to biopsy BI-RADS 4a lesions looking nonsuspicious on SWE™, and at the same time reconsidering the decision to follow-up BI-RADS 3 lesions looking suspicious on SWE™, one could expect to decrease the number of breast ultrasound false positive cases, while properly assessing the few false negative cases [21;22;27]. Several elastographic criteria have been proposed to evaluate the level of suspicion of BI-RADS 3 and 4a lesions such as the maximum stiffness within or adjacent to the lesion [21-22], the mean stiffness of the stiffest area within or adjacent to the lesion [21;27], the homogeneity of the SWE™ map [22] and the stiffness ratio between the stiffest part of the lesion and the subcutaneous fatty tissue [21] (Table 3).

| Author    | SWE™ criterion            | Suspicious level for            | Non-suspicious for BI-RADS 4a BI-RADS 3  |
|-----------|---------------------------|---------------------------------|--|
| Berg [22] | Maximum stiffness (color) | Red                             | Blue (aggressive rule)<br>Dark blue (conservative rule)                                  |
| Berg [22] | Maximum stiffness (value) | 160 kPa                         | 80 kPa (aggressive rule)   |
| Berg [22] | SWE™ map homogeneity      | Heterogeneous (aggressive rule) | Reasonably-to-very homogeneous (aggressive rule)<br>Very homogeneous (conservative rule) |
| Lee [31]  | Maximum stiffness         | N/A (color)                     | Dark blue  |
| Lee [31]  | Maximum stiffness         | N/A (value)                     | 65 kPa (aggressive rule)<br>30 kPa (conservative rule)                                   |
| Ko [27]   | Mean stiffness            | N/A (value)                     | 41.6 kPa   |
| Au [21]   | Maximum stiffness         | N/A (value)                     | 46.7 kPa   |
| Au [21]   | Mean stiffness            | N/A (value)                     | 42.5 kPa   |
| Au [21]   | Stiffness ratio           | N/A (lesion/fat)                | 3.65   |

**Table 3. List of SWE™ criteria that have been considered to improve breast ultrasound specificity and Positive Predictive Value.**

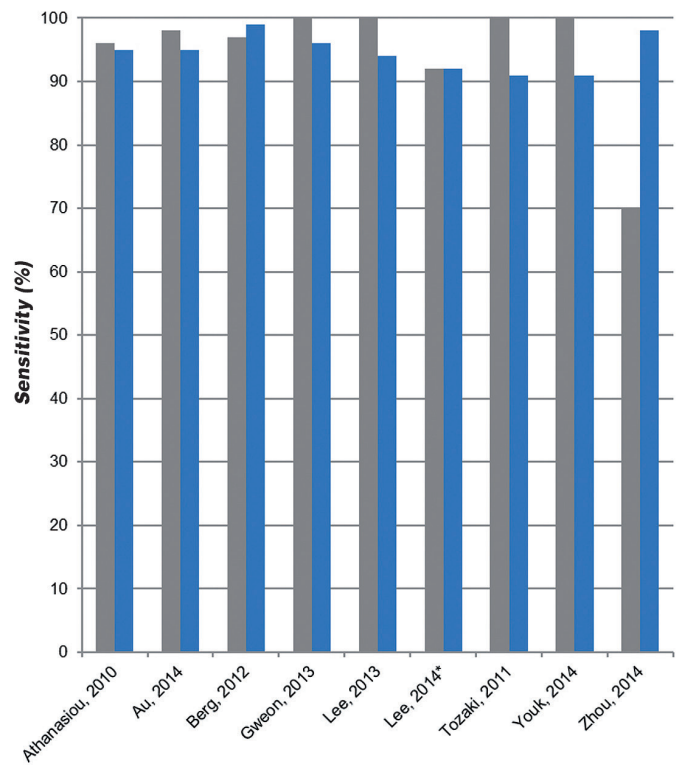
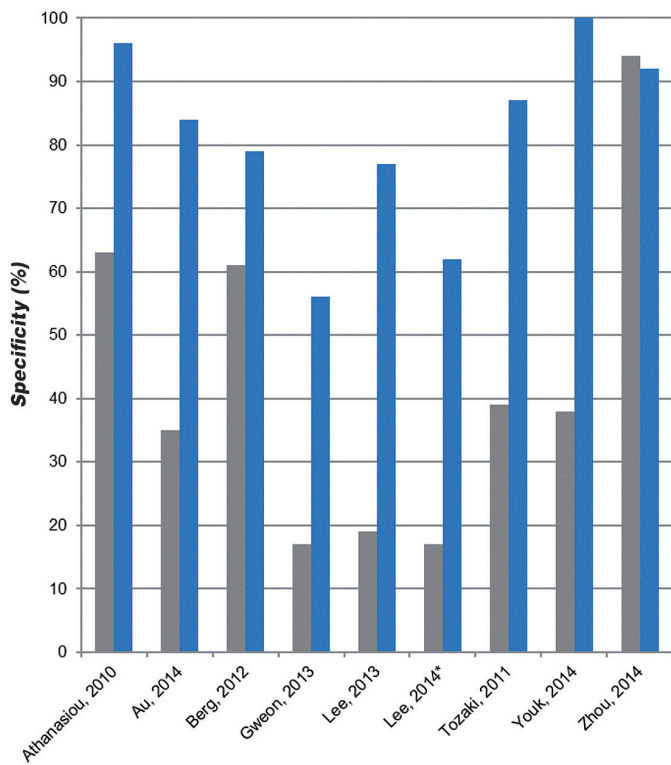


Figure 2.

Increase of diagnostic performances of breast ultrasound (gray bars) when stiffness assessment by SWE™ was combined to the BI-RADS assessment (blue bars). All studies but one reported a statistically significant increase in specificity, while there was no significant change in sensitivity. The study by Zhou et al showed contradictory results as compared to other studies probably because they used a diagnostic threshold between BI-RADS 4a and 4b for the morphological evaluation of the malignancy risk, which explains the low sensitivity, and the slight decrease in specificity after the combination of SWE™ information.

\* The study published by Lee et al in 2014 was performed on a population who underwent screening ultrasound for breast cancer. The mix of screening and diagnostic populations in Asian countries may explain the very low specificity of conventional breast ultrasound in Gweon's and Lee's reports, which appeared to be compensated by the addition of SWE™ stiffness assessment.

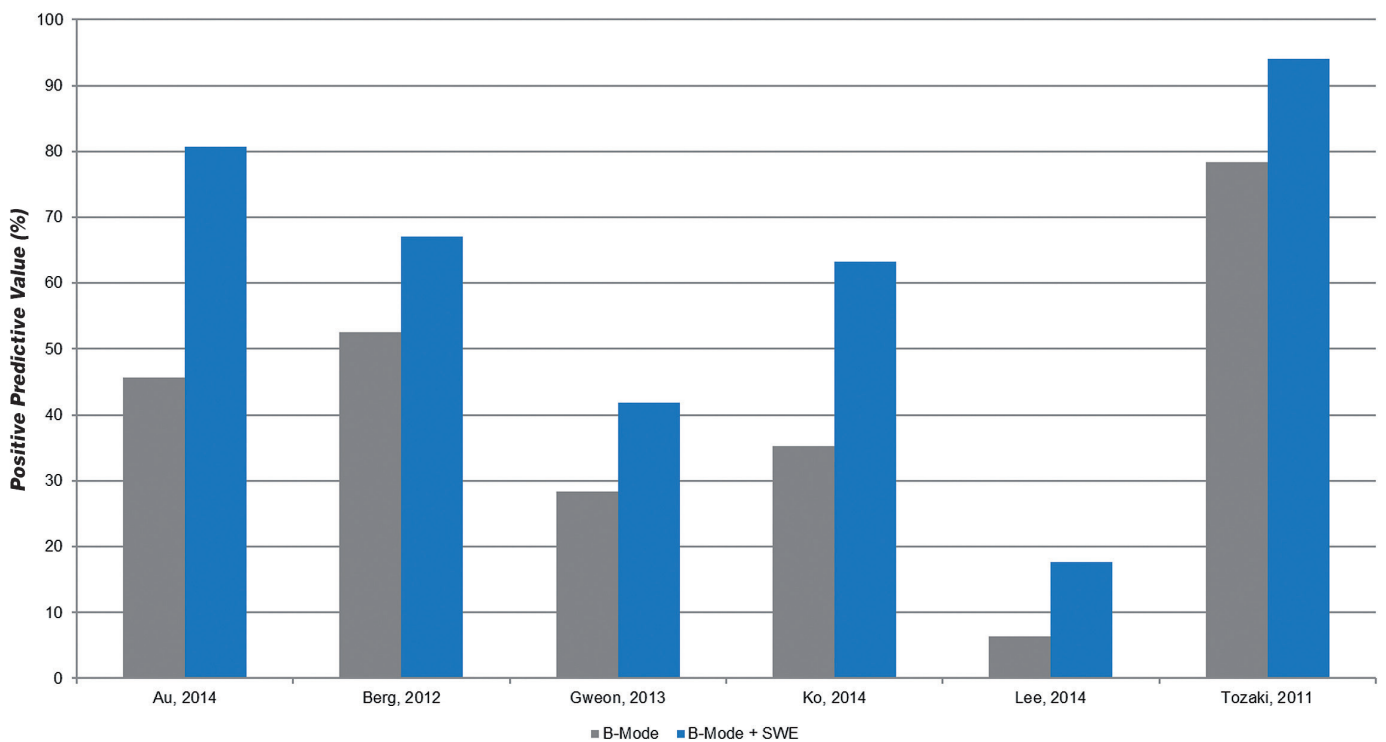


Figure 3.

Increase in Positive Predictive Value for biopsy recommendation with ultrasound, by adding SWE™ features to morphological lesions assessment.

This benefit was also demonstrated and confirmed in the context of screening ultrasound [31]. The specificity could have been increased from 17.4% for initial BI-RADS® assessment to 62% if BI-RADS 4a lesions appearing with a homogeneous dark-blue SWE™ map would have been selectively downgraded to follow-up. No change in sensitivity would have been observed (91.7%), meaning that no cancer would have been moved from biopsy to follow-up.

In mid-2013, elasticity imaging has been added to the 2nd edition of the BI-RADS® lexicon for ultrasound imaging [2], while in 2014, the Korean Society of Ultrasound in Medicine (KSUM) published its “Practice guideline for the performance of breast ultrasound elastography”. The society recommended that BI-RADS 4a lesions that are negative on elastography could be considered for short-term follow-up instead of biopsy, while elastography positive BI-RADS 3 lesions could be considered for biopsy [32].

In addition, elastography-negative BI-RADS 3 lesions could be considered for routine instead of initial short-term follow-up.

## 4.2 Improved sensitivity of breast ultrasound

SWE™ evaluation of breast lesions has also shown to improve the ability of ultrasound imaging to properly detect breast cancer within the characterization framework. Using a threshold of 50 kPa, Evans et al achieved a significant increase in both sensitivity and NPV of breast ultrasound, from 95% to 100% and from 90% to 100% respectively, by considering biopsy for masses that would be either scored BI-RADS 4 to 5 or with a mean stiffness over 50 kPa [10].

Looking at lesions that are usually categorized as “low suspicion masses” on ultrasound, i.e. which appear oval, circumscribed, with no other suspicious sign, Berg et al found that the addition of maximum stiffness could help improve significantly the sensitivity of ultrasound from 0% to 100% [22]. Although this conclusion must be taken with great caution due the limited number of cancers in this subgroup of breast masses (only 4 in this study), there seems to be a high potential for SWE™ imaging and stiffness measurement to properly identify the most suspicious masses within the subset of “low suspicion lesions”.

In patients undergoing second-look ultrasound after positive magnetic resonance imaging (MRI) findings, SWE™ imaging helped to perform biopsy under ultrasound guidance by improving the visualization of subtle or difficult-to-target breast lesions [33]. Of the 96 BI-RADS 4 and 5 lesions on dynamic contrast-enhanced MRI that were recruited, 29 were malignant. Twenty-two of these cancers could be properly targeted for ultrasound-guided biopsy during second-look ultrasound exam, of which 5 invasive carcinomas (4 ductal and 1 lobular) that could only be targeted thanks to SWE™. When added to second-look ultrasound after MRI, SWE™ increased the sensitivity of breast ultrasound by 29% and helped target cancers for ultrasound-guided biopsy.

---

## 5. Information for Treatment Planning and Monitoring

### 5.1 Pre-operative assessment of breast cancer size

Ultrasound imaging usually stands as the imaging modality that underestimates the most the size of breast cancers. The extension of peritumoral stiffness beyond 3 mm from the lesion borders seen on ultrasound has been proven to be associated with this underestimation of the histological cancer size [34]. In this retrospective study, 86 patients undergoing breast conserving surgery for breast cancer were analyzed. The cancer size was underestimated by more than 5 mm in 40% of cases using grayscale ultrasound alone. This rate could be reduced to 12% by adding the size of peritumoral stiffness seen on SWE™ maps, thus leading to an accurate measurement of lesion size, within 2 mm of the actual histological size, in 53.5% of the cases. In another study, the histologic size of 29 cancers after excision could be compared to that measured on grayscale images and stiffness maps.

B-mode size was significantly lower than histologic size on average (13.5 mm versus 17.0 mm;  $p < 0.001$ ), while no significant difference could be observed between stiffness map size (18.5 mm) and histologic size ( $p = 0.698$ ) [35].

## 5.2 Cancer aggressiveness and prognostic information

Prognostic information is usually determined from histological and pathological analysis of biopsy samples, and mainly includes cancer sub-typing and immunohistochemical phenotyping.

Significant relationships have been demonstrated by univariate analysis between stiffness of breast cancer

and prognostic factors, such as cancer invasive size, lympho-vascular invasion, lymph nodes involvement and histologic cancer grade, thus providing important prognostic information at the stage of diagnostic imaging. However, these factors should be considered depending on the size of the mass, which was demonstrated to correlate as well with stiffness values in benign and malignant masses (Table 4) [23-24;37].

| Author     | Nb  | <10 mm        | 10-19 mm       | 20-29 mm or >20 mm | >30 mm       | P value |
|------------|-----|---------------|----------------|--------------------|--------------|---------|
| Chang [37] | 337 | 90.1+/-48.7   | 127.2+/-50.3   | 165.6+/-53.3       | N/A          | <0.0001 |
| Lee [38]   | 30  | N/A           | 112.1+/-59.4   | 173.2+/-66.4       | 214.4+/-68.9 | 0.071   |
| Ganau [39] | 216 | 105.12+/-64.1 | 123.45+/-54.62 | 148.04+/-70.51     | N/A          | 0.005   |
| Evans [40] | 101 | 64+/-23       | 129+/-66       | 156+/-45           | N/A          | <0.0001 |

Table 4. Average and standard deviation of breast cancer maximum stiffness as a function of tumor size.

### 5.2.1 Stiffness and histo-pathologic severity

Maximum stiffness of breast masses has been shown to correlate with their histo-pathologic severity [23].

In this study performed on a prototype equipment, on which stiffness values were capped at 180 kPa per equipment design, invasive cancers were reported to be at the highest end of the stiffness range, with a median value of 180 kPa (range: 138-180 kPa).

Lower median stiffness values were then found for ductal carcinomas in situ (DCIS) at 126 kPa (range: 71-180 kPa), followed by high-risk lesions (median: 71 kPa; range: 32-172 kPa), and usual benign lesions, including fibrocystic changes, fibrosis and fibroadenomas (median: 45 kPa; range: 27-85 kPa).

Lipomas were reported to be on the lowest end of the stiffness range, with a median value of 14 kPa (range: 8-15 kPa). Authors concluded that maximum stiffness values measured by SWE™ can be considered as a predictor of histopathologic severity.

The difference observed between invasive cancers and DCIS was confirmed by other works (Table 5 and Figure 4).

This finding suggests that biopsy-proven DCIS could very likely be upgraded to IDCs at surgical excision if their maximum stiffness reaches 180 kPa or more. Per Table 5, invasive lobular carcinomas (ILC) seem to be of similar stiffness as IDC (Figure 5), although in some publications, they were reported to be stiffer [24;38; 40-41]. In their work published in 2016, Brkljačić and al confirmed on a homogeneous group of 40 pure ILC that they were slightly, although significantly, stiffer than IDC in general (average EMax values of 210.6 kPa versus 191.6 kPa, respectively,  $p < 0.005$ ), the difference being even more obvious in lesions of or below 1.5 cm in size (average EMax values of 198.3 kPa versus 176.2 kPa, respectively,  $p < 0.005$ ).

No significant difference could be observed between ILC and IDC over 1.5 cm in size [41]. Mucinous cancers are generally considered to be soft tumors, however strain elastography tended to show that they were stiffer than the surrounding breast tissue [42]. Average stiffness values of mucinous cancers measured with SWE™ were reported to range from 95 kPa to 270 kPa. Most authors found values higher or like those of IDCs, except one study which concluded that they were softer than other cancer subtypes [40] (Table 6).

| Author     | DCIS                    | IDC               | ILC                      |
|------------|-------------------------|-------------------|--------------------------|
| Au [36]    |                         |                   | 270.65+/-41.51 (241-300) |
| Chang [24] |                         |                   | 190.9 (N/A)              |
| Chang [37] | 177.2 (medullar) (N/A)  | 95.5+/-65.4 (N/A) | 182.9+/-50.8 (N/A)       |
| Evans [40] | 96+/-89 (tubular) (N/A) | 105+/-40 (N/A)    |                          |
| Ganau [39] | 122.35+/-50.94 (N/A)    |                   | 94.81+/-19.58 (N/A)      |
| Lee [38]   |                         | 195.9 (N/A)       |                          |

Table 6. Average, standard deviation and range of maximum stiffness values of other breast cancer subtypes.

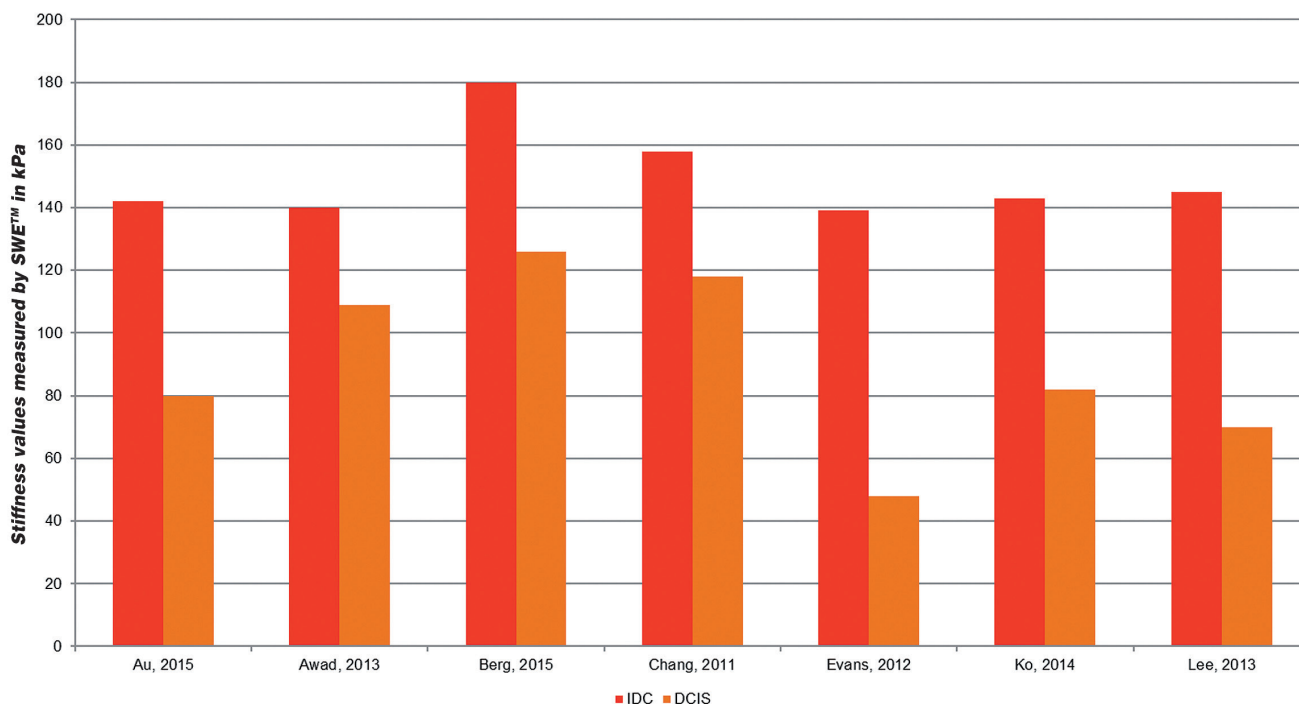


Figure 4. Average maximum stiffness values of invasive ductal carcinomas (red) and ductal carcinomas in situ (orange) reported in 6 peer-reviewed publications.

| Author         | DCIS                   | IDC                     | ILC                     |
|----------------|------------------------|-------------------------|-------------------------|
| Au [36]        | 95.36+/-72.11 (37-221) | 169.76+/-86.94 (20-300) | 300.0 (N/A)             |
| Berg [23]      | 126 (IQR=71-180)       | 180 (IQR=162-180)       | 180 (IQR=124-180)       |
| Chang [24]     | 117.8+/-54.72 (47-193) | 157.5+/-57.07 (58-300)  | 169.5+/-61.06 (108-284) |
| Chang [37]     | N/A                    | 147.9+/-57.04 (N/A)     | 149+/-51.7 (N/A)        |
| Evans [40]     | N/A                    | 139+/-56 (N/A)          | 181+/-67 (N/A)          |
| Ganau [39]     | N/A                    | 130.92+/-65.68 (N/A)    | 136.06+/-71.24 (N/A)    |
| Ko [27]        | 82.+/-50.3 (N/A)       | 142.8+/-86.4 (N/A)      | N/A                     |
| Brkljacic [41] | N/A                    | 191.6+/-41.3 (N/A)      | 210.6+/-35.5 (N/A)      |
| Lee [43]       | 79.23+/-42.67 (16-107) | 182.21+/-86.35 (25-300) | N/A                     |

Table 5. Average, standard deviation and range of maximum stiffness values of main breast cancer subtypes.

| Author     | Nb cancers | LVI<0        | LVI>0        | P value |
|------------|------------|--------------|--------------|---------|
| Au [36]    | 72         | 147+/-82.2   | 209+/-53.3   | 0.004   |
| Evans [40] | 101        | 133+/-60     | 154+/-56     | 0.0077  |
| Youk [45]  | 161        | 138.3+/-44.6 | 187.7+/-58.3 | <0.0001 |

Table 7. Average and standard deviation of breast cancer maximum stiffness as a function of lymphovascular invasion status.

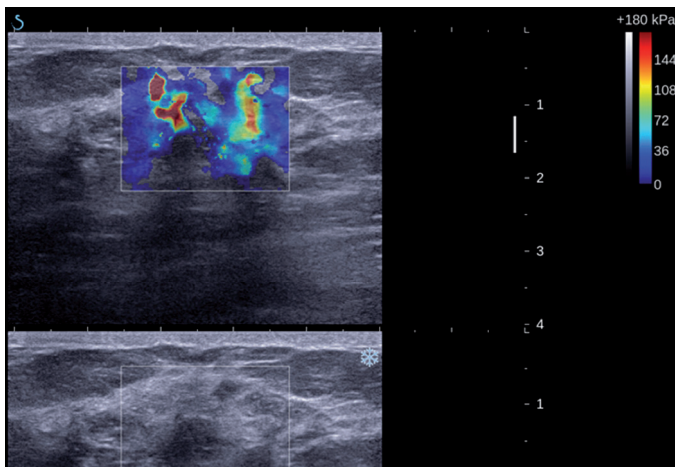


**Figure 5.** Biopsy-proven invasive lobular cancer in a 69-year-old patient. On grayscale ultrasound (bottom), the lesion appeared as hypoechoic with indistinct margins in the lower half of the box. A secondary irregular and hypoechoic area could be observed in the upper half of the box surrounded by breast glandular tissue. On SSWE imaging (top), a very heterogeneous pattern could be observed, showing a lack of SWE™ signal within the main hypoechoic lesion, increased stiffness values at its periphery (> 180 kPa), as well as next to the secondary hypoechoic area. Courtesy of B Brkljačić, MD and G Ivanac, MD, Department of Diagnostic and Interventional Radiology, University Hospital “Dubrava”, Zagreb, Croatia.

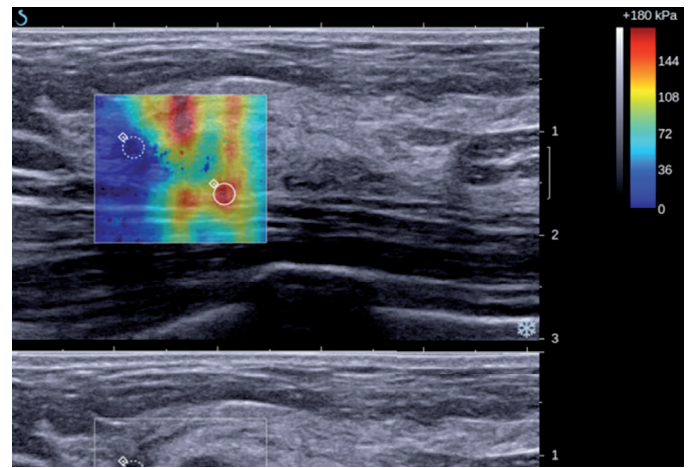


**Figure 6.** Biopsy-proven Grade 3 Invasive Ductal Carcinoma assessed with ultrasound imaging prior to core-needle biopsy. On grayscale ultrasound imaging (bottom image) the mass showed as an oval, circumscribed, hypo echoic solid mass, located at 1 o'clock and 6 cm from the nipple. The mass was scored BI-RADS 4C. The SSWE map (top image) had a highly heterogeneous appearance. The circular ROI positioned over one of the stiffest areas in adjacent tissue (solid line) measured the maximal stiffness value of 164.6 kPa. Courtesy of K. Schilling, MD, Department of Radiology, Lynn Women’s Institute Center for Breast Care, Boca Raton Regional Hospital, Boca Raton, FL, USA.

| Author     | Nb cancers | LN<0         | LN>0         | P value |
|------------|------------|--------------|--------------|---------|
| Au [36]    | 72         | 154.4+/-87.2 | 204.1+/-87.7 | 0.04    |
| Chang [37] | 337        | 144.2+/-56.9 | 158.7+/-60.2 | 0.012   |
| Evans [40] | 98         | 126+/-53     | 157+/-61     | <0.0001 |
| Lee [38]   | 30         | 127.5+/-60.4 | 197.6+/-72.1 | 0.005   |
| Youk [45]  | 166        | 139.5+/-46.7 | 162.3+/-53.9 | 0.018   |

**Table 8.** Average and standard deviation of breast cancer maximum stiffness as a function of axillary lymph nodes status.

| Author     | Nb cancers | Grade I        | Grade II       | Grade III            | P value |
|------------|------------|----------------|----------------|----------------------|---------|
| Au [36]    | 72         | 127.4+/-76.8   | 131.5+/-78.5   | 163.4+/-77.9 (trend) | 0.247   |
| Chang [37] | 337        | 117.2+/-53     | 132+/-57.7     | 165+/-52.4           | <0.0001 |
| Evans [40] | 101        | 88+/-62        | 143+/-55       | 147+/-58             | <0.0001 |
| Ganau [39] | 216        | 112.09+/-55.35 | 141.95+/-73.76 | 130.31+/-55.92       | NS      |
| Youk [45]  | 159        | 110.5+/-36.1   | 149.7+/-41.5   | 185.5+/-52.7         | <0.0001 |

**Table 9.** Average and standard deviation of breast cancer maximum stiffness as a function of histologic grade.

| Author      | Nb  | ER+          | HER2+          | TNBC           | P value |
|-------------|-----|--------------|----------------|----------------|---------|
| Chang [37]a | 337 | 136.9+/-57.2 | 160+/-56.2     | 169.1+/-48.5   | <0.0001 |
| Ganau [39]  | 216 | 121.6+/-44.0 | 107.88+/-42.34 | 125.82+/-49.08 | Ns      |
| Youk [45]   | 166 | 139.6+/-47.8 | 155.4+/-53.2   | 163.1+/-47.6   | N/a     |

**Table 10.** Average and standard deviation of breast cancer maximum stiffness as a function of immuno-histochemical phenotype. ER+: cancer cells overexpressing Estrogen Receptors; HER2+: cancer cells overexpressing Human Epidermal growth factor Receptor 2; TNBC: triple negative breast cancers.

## 5.2.2 Stiffness and cancer aggressiveness

A significant correlation has been demonstrated between breast cancer maximum stiffness and increased lesion vascularization (Table 7), metastatic lymph nodes (Table 8), and histological grade (Table 9). As an example, Figure 6 illustrates a Grade 3 IDC presenting with a high maximal stiffness value of 164.6 kPa.

Breast cancer maximum stiffness has been demonstrated by Evans et al to be an effective predictor of lymph node metastasis, especially when associated with tumor size, tumor type and vascular invasion [44]. Several works reported increased stiffness values for high histological grade cancers (Table 9), however, Berg et al found the opposite conclusion for masses equal or below 9 mm in size, which could be explained by central necrosis in high-grade cancers [23].

## 5.2.3 Stiffness and immuno histochemical phenotype

Cancers overexpressing Estrogen Receptors (ER+) appeared to be significantly softer than ER- cancers; no significant differences could be demonstrated depending on the overexpression or not of Human Epidermal growth factor Receptor 2 (HER2+), although a trend may exist. Triple negative breast cancers (TNBC) were found to be significantly stiffer than ER+ and HER2+ cancers in some experiences (Figure 7) [38;46], whereas in others, no difference could be found [40] (Table 10). Two studies concentrated on TNBC. They reported varying or benign SWE™ features, for this subtype of breast cancers which is already known to appear with benign ultrasound signs [46-47]. Džoić Dominković et al reported an average maximum stiffness of 166.85±/64.71 kPa for TNBC versus 226.63±/54.1 kPa for other invasive cancers ( $p < 0.05$ ) and concluded that TNBC were softer than other more common types of invasive cancers [46]. Boisserie-Lacroix et al evaluated the global radiological signs of TNBC and reported stiffness values for 17 cases, ranging from 0 to 232 kPa [47].

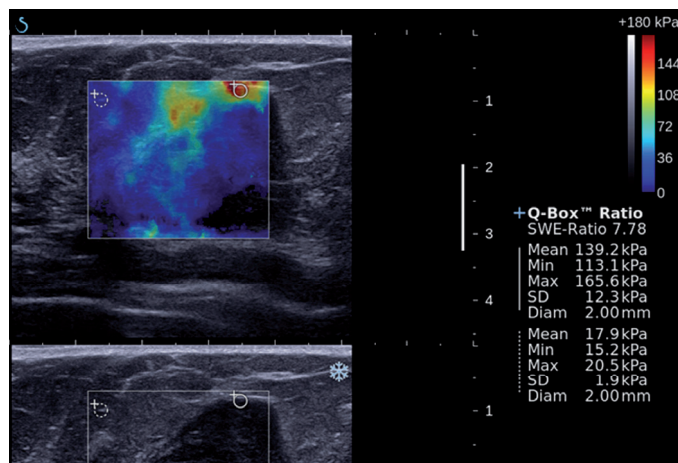


Figure 7.

**Biopsy-proven Grade 3 Invasive Ductal Carcinoma assessed with A biopsy-proven triple negative breast cancer in a 66-year-old patient, showing as a large 25 x 30 mm solid mass on grayscale ultrasound (bottom). On SSWE imaging, highest stiffness values appeared to be localized in the periphery of the mass. The maximal stiffness value measured was 165.6 kPa, and stiffness ratio between the mass and the fatty reference tissue was 7.78. Courtesy of B Brkljačić, MD and G Ivanac, MD, Department of Diagnostic and Interventional Radiology, University Hospital "Dubrava", Zagreb, Croatia.**

## 5.3 Monitoring and prediction of response to neo-adjuvant chemotherapy

In patients with invasive breast cancer undergoing preoperative neo-adjuvant chemotherapy (NACT), significant correlations have been reported between pre-operative stiffness values and responsiveness to treatment. Pre-operative stiffness measured on 25 patients correlated with post-treatment percentage of residual cellularity (Pearson's  $R=0.35$ ;  $p < 0.0001$ ) and with the residual cancer burden score (Pearson's  $R=0.23$ ;  $p=0.004$ ), which assesses the response to NACT by taking into consideration the post-NACT primary tumor dimensions, the cellularity of the tumor bed and the axillary lymph node burden [48].

The proof of concept for using SWE™ measurements to monitor breast cancers during NACT started with a feasibility study on 10 patients. In this study, the use of 3D-SWE™ during treatment proved to be useful to monitor its effectiveness. Decrease in tumor stiffness and heterogeneity was associated with response to treatment [49].

This benefit was confirmed by another study completed on 71 patients undergoing NACT for grade II and III invasive breast cancers before surgery. Eighty-six percent of patients were found to have residual cancer after completion of NACT and showed on average higher maximum stiffness values than those without residual cancer ( $116.0 \pm 74.1$  kPa versus  $26.4 \pm 21.0$  kPa;  $p < 0.001$ ).

The area under the ROC curve for B Mode US + SWE™ to predict residual cancer was significantly higher than the one for B Mode ultrasound only (0.877 versus 0.702;  $p=0.014$ ), while at the same it showed no significant difference with that of dynamic contrastenhanced MRI (0.939;  $p=0.147$ ), which is known to assess the most accurately tumor response to NACT [50].

---

## 6. Conclusion

**Owing to its correlation with cancer risk, real-time mapping of breast lesions stiffness has proven to produce important information to breast physicians that can improve the global management patients with breast lesions. It can significantly improve the positive predictive value of biopsy recommendation for probably benign and low suspicion breast lesions on ultrasound, while maintaining (or even increasing) the sensitivity of breast ultrasound.**

**This benefit has been demonstrated both in the diagnostic and screening settings. The addition of SWE™ evaluation of breast lesions also increases the inter-observer agreement on their global cancer risk assessment with ultrasound, thanks to its “almost perfect” intra-operator repeatability and high inter-observer reproducibility. The evaluation of breast cancers with SWE™ seem to contribute to defining more appropriate management strategies thanks to more accurate cancer size measurements, to correlation with cancer aggressiveness and response to neo-adjuvant chemotherapy treatment.**

## 7. References

- 1- Berg WA, Gutierrez L, NessAiver MS, et al. Diagnostic accuracy of mammography, clinical examination, US, and MR imaging in preoperative assessment of breast cancer. *Radiology* 2004;233:830-849.
- 2- Mendelson EB, Böhm-Vélez M, Berg WA, et al. ACR BI-RADS® Ultrasound. In: ACR BI-RADS® Atlas, Breast Imaging Reporting and Data System. Reston, VA, American College of Radiology; 2015.
- 3- Parker SH, Jobe WE, Dennis MA, et al. US-guided automated large-core breast biopsy. *Radiology* 1993;187:507-511.
- 4- Berg WA, Blume JD, Cormack JB, et al. Combined screening with ultrasound and mammography vs mammography alone in women at elevated risk of breast cancer. *JAMA*. 2008 May 14;299(18):2151-63. doi: 10.1001/jama.299.18.2151. Erratum in: *JAMA*. 2010 Apr 21;303(15):1482.
- 5- Ohuchi N, Suzuki A, Sobue T, et al. Sensitivity and specificity of mammography and adjunctive ultrasonography to screen for breast cancer in the Japan Strategic Anti-cancer Randomized Trial (J-START): a randomised controlled trial. *Lancet*. 2016 Jan 23;387(10016):341-8.
- 6- Lazarus E, Mainiero MB, Schepps B, et al. BI-RADS lexicon for US and mammography: interobserver variability and positive predictive value. *Radiology* 2006;239(2):385-391.
- 7- Moorman AM, Bourez RL, de Leeuw DM, et al. Pre-operative Ultrasonographic Evaluation of Axillary Lymph Nodes in Breast Cancer Patients: For Which Group Still of Additional Value and in Which Group Cause for Special Attention? *Ultrasound Med Biol*. 2015 Aug 7. pii: S0301-5629(15)00411-1. doi: 10.1016/j.ultrasmedbio.2015.06.013.
- 8- Barr RG, Zhang Z. Effects of precompression on elasticity imaging of the breast: development of a clinically useful semiquantitative method of precompression assessment. *J Ultrasound Med*. 2012 Jun;31(6):895-902.
- 9- Cosgrove DO, Berg WA, Doré CJ, et al. Shear wave elastography for breast masses is highly reproducible. *Eur Radiol*. 2012 May;22(5): 1023-32.
- 10- Evans A, Whelehan P, Thomson K, et al. Differentiating benign from malignant solid breast masses: value of shear wave elastography according to lesion stiffness combined with greyscale ultrasound according to BI-RADS classification. *Br J Cancer*. 2012 Jul 10;107(2):224-9.
- 11- Gweon HM, Youk JH, Son EJ, et al. Clinical application of qualitative assessment for breast masses in shear-wave elastography. *Eur J Radiol*. 2013 Nov;82(11):e680-5.
- 12- Kim H, Youk JH, Gweon HM, et al. Diagnostic performance of qualitative shear-wave elastography according to different color map opacities for breast masses. *Eur J Radiol*. 2013 Aug;82(8):e326-31.
- 13- Lee SH, Cho N, Chang JM, et al. Two-view versus single-view shear-wave elastography: comparison of observer performance in differentiating benign from malignant breast masses. *Radiology*. 2014 Feb;270(2):344-53.
- 14- Youk JH, Son EJ, Gweon HM, et al. Comparison of strain and shear wave elastography for the differentiation of benign from malignant breast lesions, combined with B-mode ultrasonography: qualitative and quantitative assessments. *Ultrasound Med Biol*. 2014 Oct;40(10):2336-44.
- 15- Zhou J, Zhan W, Chang C, et al. Breast lesions: evaluation with shear wave elastography, with special emphasis on the “stiff rim” sign. *Radiology*. 2014 Jul;272(1):63-72.
- 16- Youk JH, Gweon HM, Son EJ, et al. Three-dimensional shear-wave elastography for differentiating benign and malignant breast lesions: comparison with two-dimensional shear-wave elastography. *Eur Radiol*. 2013 Jun;23(6):1519-27.

- 17- Tozaki M, Fukuma E. Pattern classification of ShearWave™ Elastography images for differential diagnosis between benign and malignant solid breast masses. *Acta Radiol.* 2011 Dec 1;52(10):1069-75.
- 18- Athanasiou A, Tardivon A, Tanter M, et al. Breast lesions: quantitative elastography with supersonic shear imaging--preliminary results. *Radiology.* 2010 Jul;256(1):297-303.
- 19- Rzymiski P, Skórzewska A, Skibinska-Zielinska M, Opala T. Factors influencing breast elasticity measured by the ultrasound Shear Wave elastography - preliminary results. *Arch Med Sci.* 2011 Feb;7(1):127-33.
- 20- Tanter M, Bercoff J, Athanasiou A, et al. Quantitative assessment of breast lesion viscoelasticity: initial clinical results using supersonic shear imaging. *Ultrasound Med Biol.* 2008 Sep;34(9):1373-86.
- 21- Au FW, Ghai S, Moshonov H, Kahn H, et al. Crystal P. Diagnostic performance of quantitative shear wave elastography in the evaluation of solid breast masses: determination of the most discriminatory parameter. *AJR Am J Roentgenol.* 2014 Sep;203(3):W328-36.
- 22- Berg WA, Cosgrove DO, Doré CJ, et al. Shearwave elastography improves the specificity of breast US: the BE1 multinational study of 939 masses. *Radiology.* 2012 Feb;262(2):435-49.
- 23- Berg WA, Mendelson EB, Cosgrove DO, et al. Quantitative Maximum Shear-Wave Stiffness of Breast Masses as a Predictor of Histopathologic Severity. *AJR Am J Roentgenol.* 2015 Aug;205(2):448-55. Chang, 2011.
- 24- Chang JM, Moon WK, Cho N, et al. Clinical application of shear wave elastography (SWE™) in the diagnosis of benign and malignant breast diseases. *Breast Cancer Res Treat.* 2011 Aug;129(1):89-97.
- 25- Chang JM, Won JK, Lee KB, et al. Comparison of shearwave and strain ultrasound elastography in the differentiation of benign and malignant breast lesions. *AJR Am J Roentgenol.* 2013 Aug; 201(2): W347-56.
- 26- Dobruch-Sobczak K, Nowicki A. Role of shear wave sonoelastography in differentiation between focal breast lesions. *Ultrasound Med Biol.* 2015;41(2):366-74.
- 27- Ko KH, Jung HK, Kim SJ, et al. Potential role of shear-wave ultrasound elastography for the differential diagnosis of breast non-mass lesions: preliminary report. *Eur Radiol.* 2014 Feb;24(2):305-11.
- 28- Youk JH, Gweon HM, Son EJ, et al. Diagnostic value of commercially available shear-wave elastography for breast cancers: integration into BI-RADS classification with subcategories of category 4. *Eur Radiol.* 2013 Oct;23(10):2695-704.
- 29- Yoon JH, Jung HK, Lee JT, Ko KH. Shear-wave elastography in the diagnosis of solid breast masses: what leads to false-negative or false-positive results? *Eur Radiol.* 2013 Sep;23(9):2432-40.
- 30- Kim MY, Choi N, Yang JH, et al. False positive or negative results of shear-wave elastography in differentiating benign from malignant breast masses: analysis of clinical and ultrasonographic characteristics. *Acta Radiol.* 2015 Oct;56(10):1155-62.
- 31- Lee SH, Chang JM, Kim WH, et al. Added value of shear-wave elastography for evaluation of breast masses detected with screening US imaging. *Radiology.* 2014 Oct;273(1):61-9.
- 32- Lee SH, Chang JM, Cho N, et al. Practice guideline for the performance of breast ultrasound elastography. *Ultrasonography.* 2014 Jan;33(1):3-10.
- 33- Plecha DM, Pham RM, Klein N, et al. Addition of shear-wave elastography during second-look MR imaging directed breast US: effect on lesion detection and biopsy targeting. *Radiology.* 2014 Sep;272(3):657-64.
- 34- Mullen R, Thompson JM, Moussa O, et al. Shear-wave elastography contributes to accurate tumour size estimation when assessing small breast cancers. *Clin Radiol.* 2014 Dec;69(12):1259-63.
- 35- Feldmann A, Langlois C, Dewailly M, et al. Shear Wave Elastography (SWE™): An Analysis of Breast Lesion Characterization in 83 Breast Lesions. *Ultrasound Med Biol.* 2015 Oct;41(10):2594-604.
- 36- Au FW, Ghai S, Lu FI, Moshonov H, Crystal P. Quantitative shear wave elastography: correlation with prognostic histologic features and immunohistochemical biomarkers of breast cancer. *Acad Radiol.* 2015 Mar;22(3):269-77.
- 37- Chang JM, Park IA, Lee SH, et al. Stiffness of tumours measured by shear-wave elastography correlated with subtypes of breast cancer. *Eur Radiol.* 2013 Sep;23(9):2450-8.
- 38- Lee SH, Moon WK, Cho N, et al. Shear-wave elastographic features of breast cancers: comparison with mechanical elasticity and histopathologic characteristics. *Invest Radiol.* 2014 Mar;49(3):147-55.
- 39- Ganau S, Andreu FJ, Escribano F, et al. Shear-wave elastography and immunohistochemical profiles in invasive breast cancer: evaluation of maximum and mean elasticity values. *Eur J Radiol.* 2015 Apr;84(4):617-22.
- 40- Evans A, Whelehan P, Thomson K, et al. Invasive breast cancer: relationship between shear-wave elastographic findings and histologic prognostic factors. *Radiology.* 2012 Jun;263(3):673-7.
- 41- Mori M, Tsunoda H, Kawachi N, et al. Elastographic evaluation of mucinous carcinoma of the breast. *Breast Cancer.* 2012 Jan;19(1):60-3.
- 42- Brkljačić B, Divjak E, Tomasović-Lončarić Č, et al. Shearwave sonoelastographic features of invasive lobular breast cancers. *Croat Med J.* 2016;57:42-50.
- 43- Lee EJ, Jung HK, Ko KH, et al. Diagnostic performances of shear wave elastography: which parameter to use in differential diagnosis of solid breast masses? *Eur Radiol.* 2013 Jul;23(7):1803-11.
- 44- Evans A, Rauchhaus P, Whelehan P, et al. Does shear wave ultrasound independently predict axillary lymph node metastasis in women with invasive breast cancer? *Breast Cancer Res Treat.* 2014 Jan;143(1):153-7.
- 45- Youk JH, Gweon HM, Son EJ, et al. Shear-wave elastography of invasive breast cancer: correlation between quantitative mean elasticity value and immunohistochemical profile. *Breast Cancer Res Treat.* 2013 Feb;138(1):119-26.
- 46- Džoić Dominković M, Ivanac G, Kelava T, Brkljačić B. Elastographic features of triple negative breast cancers. *Eur Radiol.* 2015 Aug 1.
- 47- Boisserie-Lacroix M, Mac Grogan G, Debled M, et al. Radiological features of triple-negative breast cancers (73 cases). *Diagn Interv Imaging.* 2012 Mar;93(3):183-90.
- 48- Evans A, Armstrong S, Whelehan P, et al. Can shear-wave elastography predict response to neoadjuvant chemotherapy in women with invasive breast cancer? *Br J Cancer.* 2013 Nov 26;109(11):2798-802.
- 49- Athanasiou A, Latorre-Ossa H, Criton A, et al. Feasibility of Imaging and Treatment Monitoring of Breast Lesions with Three-Dimensional Shear Wave Elastography. *Ultraschall Med.* 2015 Mar 5.
- 50- Lee SH, Chang JM, Han W, et al. Shear-Wave Elastography for the Detection of Residual Breast Cancer After Neoadjuvant Chemotherapy. *Ann Surg Oncol.* 2015 Dec;22 Suppl 3:376-84.

supersonicimagine.com

## SuperSonic Imagine

For more information contact:

+33 (0)4 42 99 24 24

contacts@supersonicimagine.com



Indications for Use: The SuperSonic Imagine Aixplorer MACH® range ultrasound diagnostic systems and transducers are intended for general purpose pulse echo ultrasound imaging, soft tissue viscoelasticity imaging and Doppler fluid flow analysis of the human body. The Aixplorer MACH® ultrasound diagnostic systems are indicated for use in the following applications, for imaging and measurement of anatomical structures: Abdominal, Small Organs, Musculoskeletal, Superficial Musculoskeletal, Vascular, Peripheral Vascular, Intraoperative, OB-GYN, Pelvic, Pediatric, Transrectal, Transvaginal, Urology, Neonatal/Adult Cephalic and Non-invasive Cardiac. In addition, the SuperSonic Imagine Aixplorer MACH® ultrasound diagnostic systems and associated transducers are intended for: measurements of abdominal anatomical structures; measurements of broadband shear wave speed, and tissue stiffness in internal structures of the liver and the spleen; measurements of brightness ratio between liver and kidney; visualization of abdominal vascularization, microvascularization and perfusion; quantification of abdominal vascularization and perfusion. The shearwave speed, beam attenuation, viscosity and stiffness measurements, the brightness ratio, the visualization of vascularization, microvascularization and perfusion, the quantification of vascularization and perfusion may be used as an aid to clinical management of adult and pediatric patients with liver disease. It is intended for use by licensed personnel qualified to direct the use of the medical ultrasound devices. CE certificate no. 26415, FDA cleared K180572.

©2020 Hologic Inc., All rights reserved. Hologic, SuperSonic, Aixplorer, Aixplorer MACH, ShearWave SWE and associated logos are trademarks and/or registered trademarks of Hologic, Inc., and/or its subsidiaries in the United States and other countries. This information is intended for medical professionals in the U.S. and other markets and is not intended as a product solicitation or promotion where such activities are prohibited. Because Hologic materials are distributed through websites, eBroadcasts and tradeshows, it is not always possible to control where such materials appear. For specific information on what products are available for sale in a particular country, please contact your local Hologic representative.